IJISET - International Journal of Innovative Science, Engineering & Technology, Vol. 3 Issue 6, June 2016
ISSN (Online) 2348 – 7968 | Impact Factor (2015) - 4.332
www.ijiset.com

Synthesis and Characterization of Titanium Dioxide Nanostructures based Photocatalysts for degradation of Rose Bengal

Vandana Chaudhary and Sudesh Chaudhary*

Center of Excellence for Energy and Environmental Studies, D.C.R. University of Science & Technology, Murthal (Sonepat) Haryana, 131039 (INDIA)

Abstract

In this paper, we report a novel surfactant mediated hydrothermal method for the synthesis of flower like TiO_2 nanostructures. The synthesized TiO_2 nanostructures were characterized by X-ray diffraction (XRD), Field emission scanning electron microscopy (FESEM), Fourier transforms infrared spectroscopy (FTIR), and UV-Vis spectroscopy. The effect of hydrothermal time (HT) on TiO_2 towards degradation efficiency of photocatalyst has been studied. It was observed that the size of nanoparticles, band-gap energy and photocatalytic activity of TiO_2 depend on hydrothermal time. The TiO_2 nanoparticles synthesized at hydrothermal time of 24 h follows first-order kinetics and indicated the highest photoreactivity towards Rose Bengal (RB). The effect of various parameters such as initial dye concentration, catalyst loading, pH of the medium, on the decolorization and photo degradation of RB also has been investigated.

Keywords: Titanium oxide, Surfactant, Photocatalysis, Rose Bengal.

***Corresponding Author:**

E-mail: 15.ritumalik.08@gmail.com

Introduction

The growth of industry worldwide has tremendously increased the generation and accumulation of waste by products. In general, the production of useful products has been focused on and the generation of waste by products has been largely ignored. This has caused severe environmental problems that have become a major concern. Researchers all over the world have been working on various approaches to address this issue. Photoinduced processes have been studied and various applications have been developed. One important technique for removing industrial waste is the use of light energy and particles sensitive to this energy to mineralize waste which aids in its removal from solution. Titanium dioxide (TiO_2) is considered very close to an ideal semiconductor for photocatalysis because of its high stability, low cost and safety toward both humans and the environment.

In 1964, Kato et al. published their work on the photocatalytic oxidation of tetralin by a TiO_2 suspension, which was followed by McLintock et al. investigating the photocatalytic oxidation of ethylene and propylene in the presence of oxygen adsorbed on TiO_2 [1,2]. However, the most important discovery that extensively promoted the field of photocatalysis was the “Honda-Fujishima Effect” first described by Fujishima and Honda in 1972 [3]. This well-known chemical phenomenon involves electrolysis of water, which is related to photocatalysis. Photoirradiation of a TiO_2 single crystal electrode immersed in an aqueous electrolyte solution induced the evolution of oxygen from the TiO_2 electrode and the evolution of hydrogen from a platinum counter electrode when an anodic bias was applied to the TiO_2 working electrode. [4]. In 1978, the first organic photosynthetic reaction was presented as an alternative photoinduced Kolbe reaction which opened the field of photosynthetic reaction [5]. In 1983, Ollis and coworker showed the extent of adsorption of several chlorinated hydrocarbons in terms of the Langmuir adsorption isotherm [6]. In 1986, Fujishima et al. used TiO_2 for photokilling tumor cells. In 1995, Fujishima et al. found that

TiO_2 films coated with certain amount of silica acquired superhydrophilic properties after irradiation with UV light [7]. In 1998, Wang et al. developed highly hydrophilic TiO_2 surfaces with excellent anti-fogging and self-cleaning properties [8]. In 2002, Watson et al. used the sol-gel technique to coat magnetic particles with TiO_2, producing a novel magnetic photocatalyst that was easy to separate from a slurry-type photoreactor by application of an external magnetic field [9]. In 2005, Sreethawong et al. synthesized nanocrystalline mesoporous TiO_2 using sol-gel techniques combined with surfactant-assisted templating and evaluated its photocatalytic activity of the evolution of hydrogen from an aqueous methanol solution [10]. In 2009, Lai and Lee revealed the ability and mechanism of photoexcited TiO_2 nanoparticles modified with folic acid to kill cells. Folic acid was bound to TiO_2 nanoparticles to provide cell targeting specificity [11]. These nanoparticles exhibited higher cytotoxicity under photoexcitation. Wang et al. synthesized TiO_2-coated magnetic silica that showed enhanced photocatalytic activity for the degradation of reactive brilliant red X-3B compared with Degussa P25 under both UV and visible light irradiation. Furthermore, the prepared composite photocatalyst had tunable magnetic properties [12].

In this work, we have synthesized TiO_2 nanostructures using sodium dodecyl sulfate as surfactant and investigated its photocatalytic performance towards degradation of RB. The degradation performance as a function of hydrothermal time of TiO_2 nanostructures was evaluated for different hydrothermal time. The result obtained at 48 h depicts the flower like morphology and degrades 96% of RB in 60 min. The effect of various parameters such as initial dye concentration, catalyst loading, pH of the medium, on the photo degradation of RhB has also been studied in this work.

2. Experimental

2.1 Preparation for photocatalyst

In a typical procedure, 1.0 g sodium dodecyl sulfate was dissolved in 60 ml of ethylene glycol by ultrasound, and then 6.8 ml $Ti(OC_4H_9)_4$ was added slowly in this solution under magnetic stirring, after that, the mixture was stirred until the clarification. 20 ml $TiCl_4$ was added dropwise into the clear solution under magnetic stirring, afterwards, the mixture was stilled until transparent solution. The solution was then placed in clean Teflon-lined stainless steel autoclaves (100 ml). The hydrothermal treatment was processed at 150 °C for different times (24, 48 and 72 h). After hydrothermal reaction, shutting the power, it was cooled naturally to room temperature. The product was washed with distilled water and alcohol for 3 times. The washed product was dried in an air at 60 °C for 12 h. Finally, the product was heated at 550 °C for 3 h in a muffle furnace. At last, the prepared photocatalysts were signed as T1, T2 and T3 for the samples synthesized at 24 h, 48 h and 72 h respectively.

2.2 Catalyst Characterization

The phase identification of the TiO_2 powders was obtained by XRD recorded using powder X-ray Diffractometer, Bruker D8 Advance with Cu Kα irradiation (λ=0.154 nm) in the 2θ range of 20–70° at scan rate of 2 °/min. The surface morphology and composition of prepared samples were investigated by FE-SEM using JEOL 6340F field emission scanning electron microscope. To examine the purity and chemical compositions, we examined the prepared SnO_2 by FTIR spectroscopy (Frontier Perkin Elmer). The spectral changes in concentration of RB during photocatalytic degradation were studied using the spectrophotometer (UV-2401 PC Shimadzu spectrophotometer).

2.3 Photocatalytic Experiment

100 ml of 10 ppm solution of Rose Bengal dye was taken in a 250 ml conical flask. Next, 0.01gm of catalyst (TiO_2) was added into this solution and the resulting mixture was stirred

vigorously (800 rpm) using a magnetic stirrer in dark for about 10 mins after which a 2 ml aliquot of the reaction mixture was taken out using a pipette. The solution was then placed in sunlight and stirred using magnetic stirrer.2 ml aliquots of the reaction mixture were taken at a regular interval during the irradiation time and centrifuged immediately to separate the suspended solids. A visible difference in the colour of the dye solution containing catalyst TiO_2 prepared via hydrothermal route was observed after 30 mins of irradiation time.

3 Results and Discussion

3.1 Characterization of TiO_2 samples

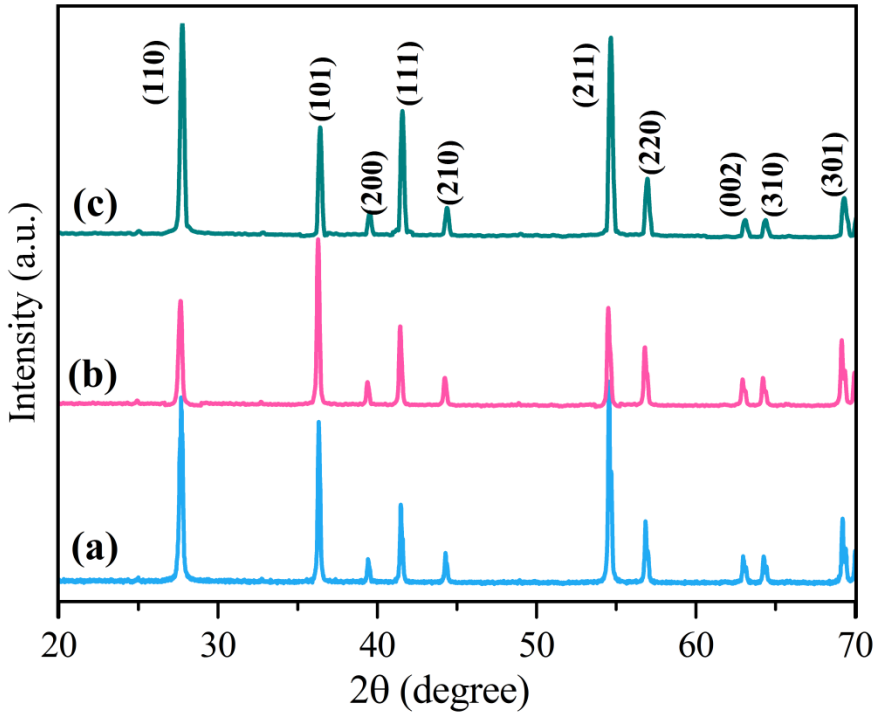

Fig. 1 XRD pattern of TiO_2 prepared for different hydrothermal treatment time **(a)** 24 h **(b)** 48 h and **(c)** 72 h

The crystal structure of TiO_2 nanoparticles were determined by glancing angle X-ray diffraction technique using CuKα (λ = 1.5418 Å) radiation. The XRD spectrum of the nanocrystalline TiO_2 prepared at different temperature as shown in Fig. 1. The XRD plots show the appearance of peaks at 25º, 37 º, 48 º, 54 º and 63 º indicating formation of TiO_2 crystalline phase [13]. The XRD peaks corresponding to (101), (004), (200), (105) and (211)

plane indicate that TiO_2 in anatase crystalline phase and show the formation of crystalline structure of nanoparticles. The size of crystal is an important factor that affects the TiO_2 photocatalytic activity. The crystalline sizes of grains were calculated by using Scherrer equation [13]. It is also observed that the increase in annealed temperature did not cause the transformation of lattice structure of TiO_2. This shows that the crystalline size is smaller for 24 h. The micro strain for peak at 2θ =25 º was calculated from Stokes and Wilson formula are shown in Table 1. The average crystalline size (*D*) of the sample prepared for different hydrothermal treatment time lies in the range of 10–18 nm.

Table 1. Experimental parameters of TiO_2 calcined at different time

Sr. No	Hydrothermal time (h)	D(nm)[a]	Microstrain[b]	Surface Area (m^2/g) [c]	Band Gap (eV)[d]	Degradation Time (min)[e]	Degradation Efficiency (%)[f]
1.	24	17.99	0.357	47	3.87	80	89.2
2.	48	10.90	0.387	81	3.76	60	96.0
3.	72	14.43	0.372	64	3.70	70	92.5

[a] $D = K\lambda/\beta \cos\theta$ where '*K*' is Scherrer's constant, 'λ' is X-ray wavelength, 'β' is full width at half-maximum and 'θ' is the diffraction angle

[b] Stokes and Wilson formula for peak at 2θ = 26.89°, $\epsilon_r = \beta/4 \tan\theta$

[c] specific surface area (SSA),$S = 6/\rho D$, where S is the specific surface area, D is the average crystallite size and ρ is the materials density.

[d] As calculated from UV-Vis Tauc plots

[e] As calculated from Fig 4.3(D)

[f] Degradation efficiency, D = (A_0-A)/A_0, where A_0 and A show initial absorbance and the final absorbance of dye sample solution

Morphology of synthesized TiO_2 nanoparticles was characterized by field-emission scanning electron microscopy (FESEM). Fig. 2(a-d) displays the FESEM images of the TiO_2 products prepared for different hydrothermal treatment time (HTT) and Fig. 2(b,c) displayed the images of the TiO_2 prepared at HTT of 48 h at different magnification. At low magnification (Fig. 2 (b)), there are a large number of porous TiO_2 nanoflowers with diameters of about 300

nm presented in FESEM image. At high magnification (Fig. 2(c)), the as-synthesized porous TiO_2 nanoflowers are composed of numerous nanosheets with diameters around 50–70 nm.

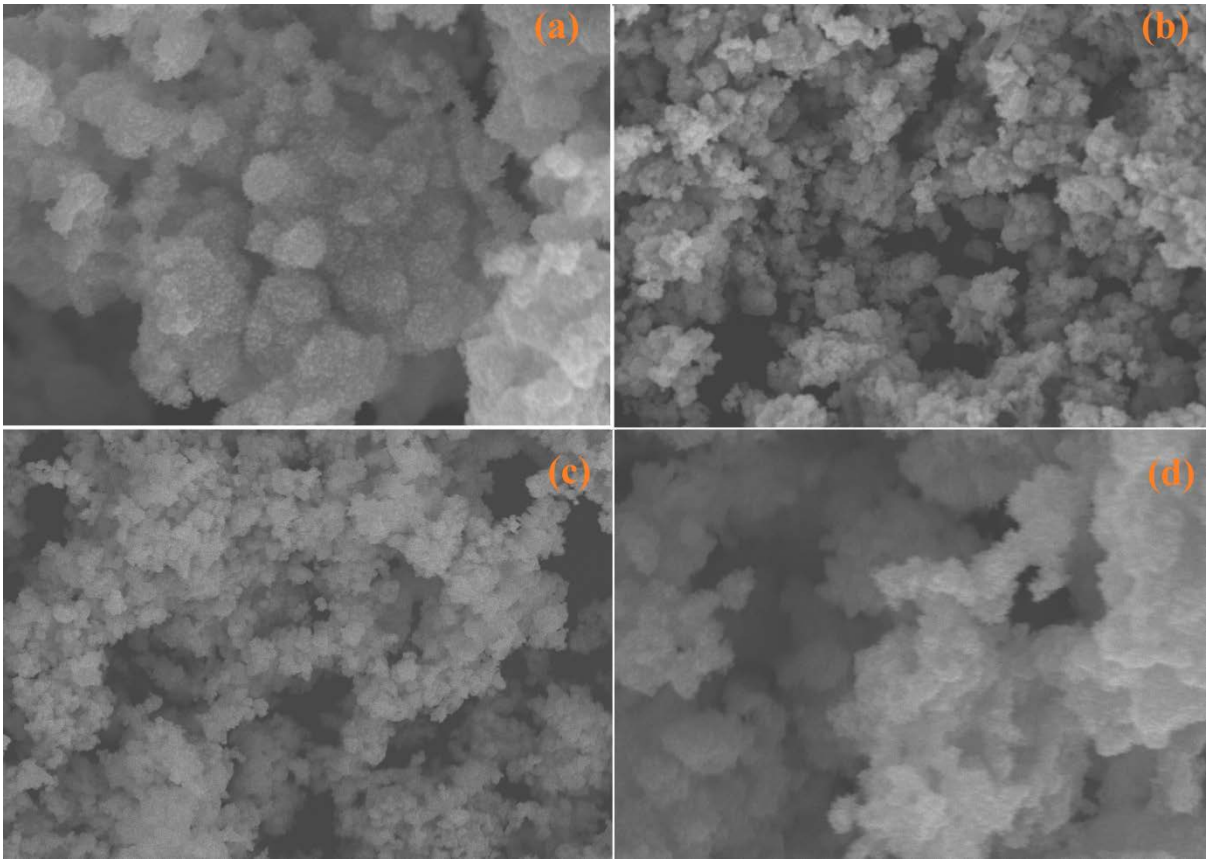

Fig. 2 FESEM images of TiO_2 prepared for different hydrothermal treatment time **(a)** 24 h **(b,c)** 48 h and **(d)** 72 h.

Fig. 3 shows the FTIR spectrum of as prepared TiO_2 nanoparticles prepared for different hydrothermal treatment time. From this spectrum, the absorption peak at 3399 cm^{-1} is attributed to the vibration of the -OH group because of the fact that the TiO_2 retain certain adsorbed water from the ambient atmosphere. The bonds observed in the region of 1176 cm^{-1} were assigned to the vibration of different types of surface hydroxyl groups [14]. The band at 635 cm^{-1} is assigned to asymmetric Ti–O–Ti stretching mode of the surface bridging oxide formed by condensation of adjacent surface hydroxyl group's vibrations [15]. The presence of such vibration in the synthesized samples confirms that TiO_2 is formed. The metal–oxygen

vibrations on the surface layer lead to the forces on the atoms as a result of the band around 635 cm^{-1}.

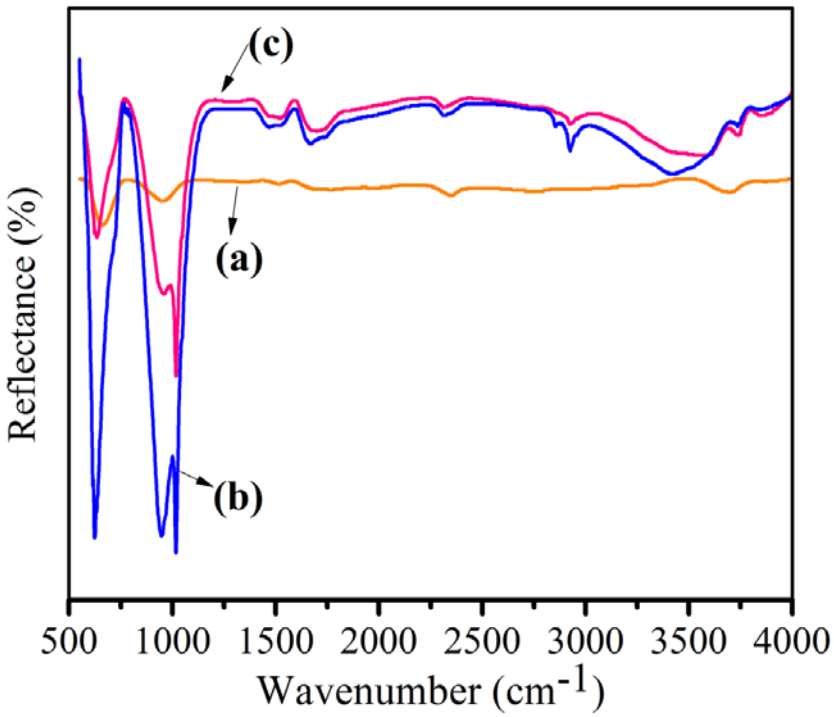

Fig. 3 FTIR specta of TiO_2 prepared for different hydrothermal treatment time **(a)** 24 h **(b)** 48 h and **(c)** 72 h.

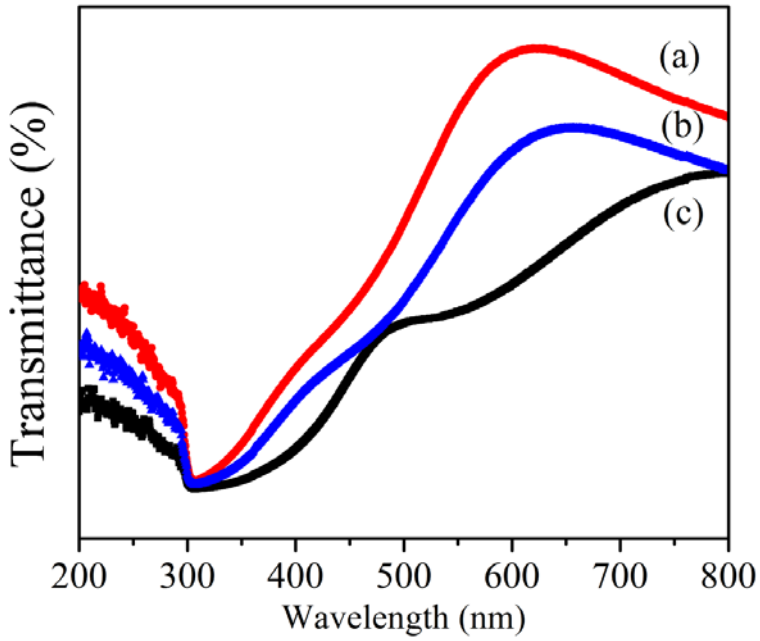

Fig. 4 UV-Vis spectra of TiO_2 nanoparticles TiO_2 prepared for different hydrothermal treatment time **(a)** 24 h **(b)** 48 h and **(d)** 72 h.

Fig. 4 shows the absorption spectra of the TiO_2 samples for different hydrothermal treatment time, which are nearly identical, indicating that the optical band gap is almost same. The fundamental absorption edge of TiO_2 located in the UV region occurs at ~325 nm [15]. The fundamental absorption edges appeared at 319.5 nm (3.87 eV), 328.5 nm (3.76 eV) and 335 nm (3.70 eV) corresponding to samples prepared for different hydrothermal treatment time 24 h, 48 h and 72 h, respectively. The sample prepared for 48 h demonstrates a little red shift due to the creation of oxygen vacancies due to which it can narrow the band gap and enhance the absorption.

3.2 Evaluation of Photocatalytic Activities

The photocatalytic activity of TiO_2 samples prepared for different hydrothermal treatment time was evaluated by monitoring the change in optical absorption of RB solution at ~553 nm during its photocatalytic decomposition process and shown in Fig. 5(a-c).The addition of TiO_2 products leads to a decrease of the absorption band of RB with time. The crystallinity of TiO_2 nanoparticles increases with increasing HTT upto 48 h, however, the TiO_2 samples prepared for 48 h (Eg = 3.76 eV) having a flower like nanostructure exhibited the outstanding photocatalytic performance among all three samples, mainly due to the specific morphology, which provide larger specific surface area than the others. We observed 89.2, 96.0 and 92.5% degradation of RhB dye by TiO_2 catalyst different hydrothermal treatment time of 24 h, 48 h and 72 h in 80, 60 and 70 min respectively.

The photocatalytic activity of semiconductor photocatalyst material is related to their corresponding energy band gap which in turn favour for the redox potential of the generated electron-hole pair in the degradation process [16]. Among the three samples prepared at different HTT, the samples prepared for 72 h shows the lowest of band gap energy (3.70 eV), however, the sample prepared for 48 h shows much enhanced photodegradation efficiency due to its unique morphology. This decrease in photocatalytic activity from sample prepared

for 72 h to sample prepared at 48 h is related to corresponding increase in particles size and thus the decrease of surface are due to agglomeration of particles in samples at HTT of 72 h. Fig 4.5(d) shows a comparison of the photocatalytic activities among TiO_2 photocatalyst treated at different calcination temperature along with test photocatalytic experiment for the pure RB solution in the absence of photocatalyst. It can be noted that a trend of photocatalytic can be attributed to UV absorption, and the products prepared for HTT of 48 h shows a red shift and shows the higher photocatalytic activity. The exciting of the nanoflowers also increases the surface area and there is more reaction place during photocatalytic process.

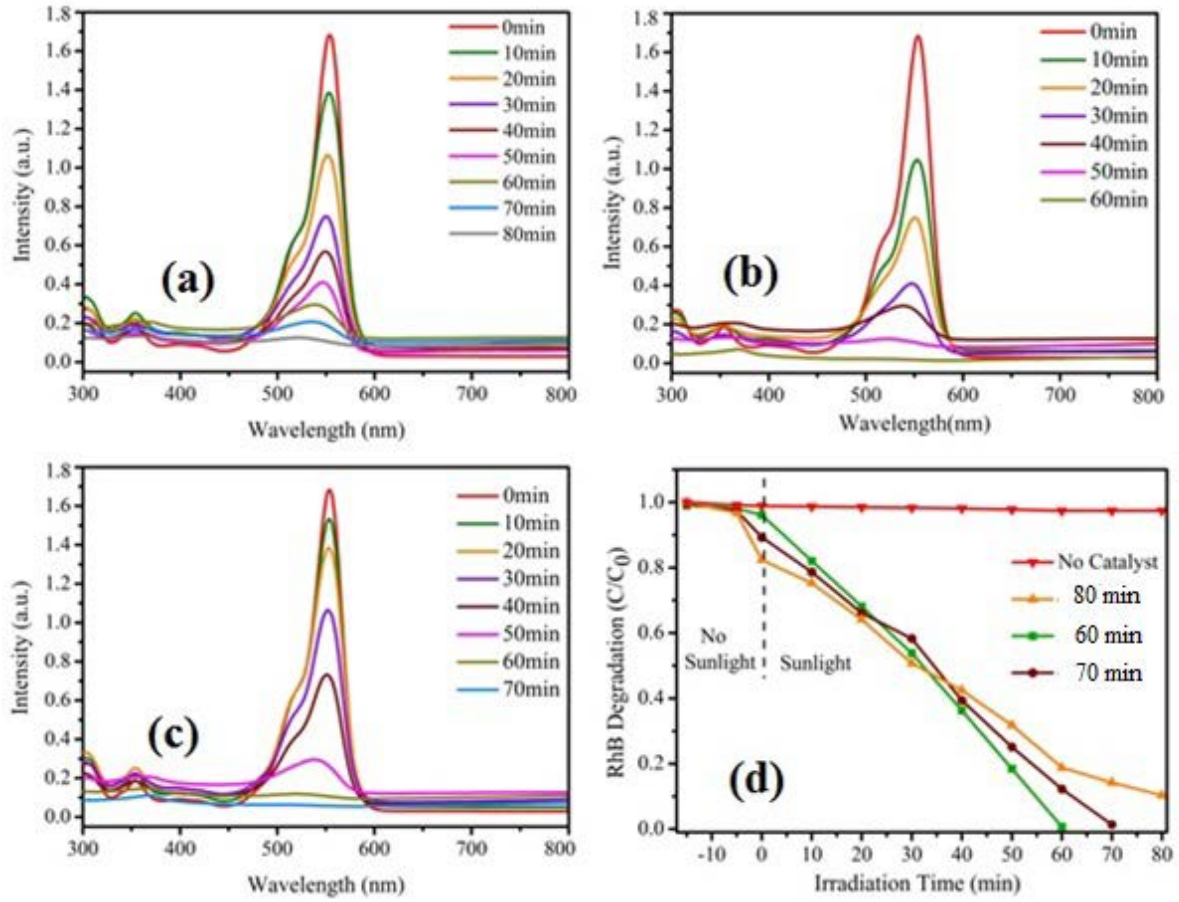

Fig 5 Photocatalytic degradation of RB solution under sunlight irradiation in the presence of TiO_2 nanoparticles prepared at (a) 24 h; (b) 48 h; (c) 72 h and (d) Comparison of the photocatalytic activities among TiO_2 photocatalyst treated at different HTT.

3.3 Mechanism of photocatalysis

A possible mechanism for photocatalytic degradation of RB and the electron transfer reaction with oxygen which are involved in the selective photo-oxidation of RB is proposed. There are

basically two ways to improve the photocatalytic efficiency of TiO_2 nanostructures [17,18]. First, the decrease in the electron-hole recombination rate which allows them to take part in the photocatalytic reaction for prolonged time, and second, optimizing the morphology and structure of the products to get more reactive species, which has significant effect on enhancing the photocatalytic efficiency. In our experiments, the photocatalytic activities of TiO_2 nanostructures may be attributed to their flower like structure. Such type of structures provide more active sites to adsorb more reactive species and O_2 and allow more effective transport for the reactant molecules to get to the active sites. This suggests that hierarchical flower like structures can improve the photon application efficiency, thus improving the efficiency of the photocatalysis [19]. In general, during photocatalytic degradation of dye molecules, hydroxyl radicals (•OH) plays an important role.

Therefore, increasing the percentage of •OH in the reaction system can immediately increase the photocatalytic efficiency. Under sunlight, the •OH radical is generated from the oxidization of H_2O by photogenerated holes (h^+) and the deoxidization of O_2occurs by the photogenerated electrons (e^-).When the TiO_2 photocatalyst is excited under visible light irradiation with energy greater than its band gap, it causes the formation of electron-hole pair on the surface of TiO_2. These photogenerated electrons and holes can recombine easily on the surface of the semiconductor. The holes and electrons thus react with dye molecules in favour of its degradation directly. In this process, the RhB can interact with the photogenerated holes in the valance band, provides a direct chemical reaction between the dye and the photocatalyst.

References

1. **S.** Kato, F. Masuo, Kogyo Kagaku Zasshi, 1964, 67, 42–50 **(1964)**.

2. S. McLintock, M. Ritchie, Trans Faraday Soc, 61, 1007–1016 **(1965)**.

3. A. Fujishima, K. Honda., Nature, 238, 37–38 **(1972)**.

4. G. N. Schrauzer, T. D. Guth, J Am Chem Soc, 99, 7189–7193 **(1977)**.

5. B. Kreutler, A. Bard, J Am Chem Soc, 100, 4317–4318, **(1978).**

6. Y. C. Hsiao, L. C. Lee, D. F. Ollist, J Catal, 82, 418–423, **(1988).**

7. A. Fujishima, J. Ohtsuki, T. Yamashita, et al., Photomed Photobiol, 8, 45–46, **(1988).**

8. R. Wang, K. Hashimoto, A. Fujishima, et al., Nature, 388, 431–432, **(1997).**

9. S. Watson, D. Beydoun, R. Amal, J Photochem Photobiol A Chemistry, 2148, 303–311, **(2005).**

10. T. Sreethawong, Y. Suzuki, S. Yoshikawa, J Solid State Chem, 178, 329–338, **(2005)**

11. Y. T. Lai, W. C. Lee, Killing of cancer cell line by photoexcitation of folic acid-modified titanium dioxidenanoparticles, J Photochem Photobiol A Chem, 204, 148–153, **(2009)**

12. C. Wang, Y. Ao, P. Wang, et al., Colloid Surf A: Physicochem Eng Aspects, 360, 184–189, **(2010)**

13. L. Mei, J. Deng, X. Yin, M. Zhang, Q. Li, E. Zhang, Z. Xu, L. Chen, T. Wang, Sens. Actuators B 166–167, 7–11, **(2012).**

14. N. Talebian, F. Jafarinezhad, Cera. Int. 39, 8311–8317, **(2013)**.

14. A. G. E. Deen, N. A. M. Barakat, K. A. Khalil, M. Motlak, H. Y. Kim, Ceram. Int. 40, 14627–14634, **(2014)**.

15. D. Chu, J. Mo, Q. Peng, Y. Zhang, Y. Wei, Z. Zhuang, Y. Li, ChemCatChem 3, 371–377, **(2011)**.

16. S. Wu, H. Cao, S. Yin, X. Liu and X. Zhang, J. Phys. Chem. C 113,17893–17898, **(2009).**

17. S. Zhenya, D. Yundi and Z. Weiying, J. Nanomater. 2008, **(2008)**.

18. Q. Kuang, Z. Y. Jiang, Z. X. Xie, S. C. Lin, S. Y. Xie, R. B. Huang, L. S. Zheng, J. Am. Chem. Soc. 127, 11777-11784, **(2005).**

19. M. Zhang, G. Sheng, J. Fu, T. An, X. Wang, X. Hu, Mater. Let. 59, 3641-3644, **(2005)**.